

Multiscattering-enhanced optical biosensor: multiplexed, non-invasive and continuous measurements of cellular processes

Volodymyr B. Koman, Christian Santschi,* and Olivier J. F. Martin

Nanophotonics and Metrology Laboratory (NAM), Swiss Federal Institute of Technology (EPFL), 1015 Lausanne, Switzerland

*christian.santschi@epfl.ch

www.nanophotonics.ch

Abstract: The continuous measurement of uptake or release of biomarkers provides invaluable information for understanding and monitoring the metabolism of cells. In this work, a multiscattering-enhanced optical biosensor for the multiplexed, non-invasive, and continuous detection of hydrogen peroxide (H_2O_2), lactate and glucose is presented. The sensing scheme is based on optical monitoring of the oxidation state of the metalloprotein cytochrome *c* (cyt *c*). The analyte of interest is enzymatically converted into H_2O_2 leading to an oxidation of the cyt *c*. Contact microspotting is used to prepare nanoliter-sized sensing spots containing either pure cyt *c*, a mixture of cyt *c* with glucose oxidase (GOx) to detect glucose, or a mixture of cyt *c* with lactate oxidase (LOx) to detect lactate. The sensing spots are embedded in a multiscattering porous medium that enhances the optical signal. We achieve limits of detection down to 240 nM and 110 nM for lactate and glucose, respectively. A microfluidic embodiment enables multiplexed and crosstalk-free experiments on living organisms. As an example, we study the uptake of exogenously supplied glucose by the green algae *Chlamydomonas reinhardtii* and simultaneously monitor the stress-related generation of H_2O_2 . This multifunctional detection scheme provides a powerful tool to study biochemical processes at cellular level.

©2015 Optical Society of America

OCIS codes: (170.1530) Cell analysis; (170.1610) Clinical applications; (170.4580) Optical diagnostics for medicine; (280.4788) Optical sensing and sensors; (290.4210) Multiple scattering; (300.1030) Absorption.

References and links

1. J. Zhang, R. E. Campbell, A. Y. Ting, and R. Y. Tsien, "Creating new fluorescent probes for cell biology," *Nat. Rev. Mol. Cell Biol.* **3**(12), 906–918 (2002).
2. A. D. Maynard, R. J. Aitken, T. Butz, V. Colvin, K. Donaldson, G. Oberdörster, M. A. Philbert, J. Ryan, A. Seaton, V. Stone, S. S. Tinkle, L. Tran, N. J. Walker, and D. B. Warheit, "Safe handling of nanotechnology," *Nature* **444**(7117), 267–269 (2006).
3. T. A. Pearson, G. A. Mensah, R. W. Alexander, J. L. Anderson, R. O. Cannon 3rd, M. Criqui, Y. Y. Fadl, S. P. Fortmann, Y. Hong, G. L. Myers, N. Rifai, S. C. Smith, Jr., K. Taubert, R. P. Tracy, and F. Vinicor, "Markers of Inflammation and Cardiovascular Disease: Application to Clinical and Public Health Practice: A Statement for Healthcare Professionals From the Centers for Disease Control and Prevention and the American Heart Association," *Circulation* **107**(3), 499–511 (2003).
4. E. A. McGlynn, S. M. Asch, J. Adams, J. Keeseey, J. Hicks, A. DeCristofaro, and E. A. Kerr, "The Quality of Health Care Delivered to Adults in the United States," *N. Engl. J. Med.* **348**(26), 2635–2645 (2003).
5. C. M. Masimirembwa, R. Thompson, and T. B. Andersson, "In Vitro High Throughput Screening of Compounds for Favorable Metabolic Properties in Drug Discovery," *Comb. Chem. High Throughput Screen.* **4**(3), 245–263 (2001).

6. S. Granick and S. I. Beale, "Hemes, Chlorophylls, and Related Compounds: Biosynthesis and Metabolic Regulation," in *Advances in Enzymology and Related Areas of Molecular Biology* (John Wiley & Sons, Inc., 2006), pp. 33–203.
7. B. A. Gregg and A. Heller, "Cross-linked redox gels containing glucose oxidase for amperometric biosensor applications," *Anal. Chem.* **62**(3), 258–263 (1990).
8. O. Lev, Z. Wu, S. Bharathi, V. Glezer, A. Modestov, J. Gun, L. Rabinovich, and S. Sampath, "Sol–Gel Materials in Electrochemistry," *Chem. Mater.* **9**(11), 2354–2375 (1997).
9. J. Tuomilehto, J. Lindström, J. G. Eriksson, T. T. Valle, H. Hämäläinen, P. Ilanne-Parikka, S. Keinänen-Kiukaanniemi, M. Laakso, A. Louheranta, M. Rastas, V. Salminen, M. Uusitupa, Z. Cepaitis, V. Moltchanov, M. Hakumäki, M. Mannelin, V. Martikkala, J. Sundvall, and M. Uusitupa; Finnish Diabetes Prevention Study Group, "Prevention of Type 2 Diabetes Mellitus by Changes in Lifestyle Among Subjects with Impaired Glucose Tolerance," *N. Engl. J. Med.* **344**(18), 1343–1350 (2001).
10. B. Åhrén and H. Larsson, "Quantification of Insulin Secretion in Relation to Insulin Sensitivity in Nondiabetic Postmenopausal Women," *Diabetes* **51**(Suppl 1), S202–S211 (2002).
11. Y. Lin, F. Lu, Y. Tu, and Z. Ren, "Glucose Biosensors Based on Carbon Nanotube Nanoelectrode Ensembles," *Nano Lett.* **4**(2), 191–195 (2004).
12. G. Strom, "The Influence of Anoxia on Lactate Utilization in Man After Prolonged Muscular Work," *Acta Physiol. Scand.* **17**(4), 440–451 (1949).
13. W. E. Huckabee, "Relationships of pyruvate and lactate during anaerobic metabolism. I. Effects of infusion of pyruvate or glucose and of hyperventilation," *J. Clin. Invest.* **37**(2), 244–254 (1958).
14. M. H. Weil and A. A. Afifi, "Experimental and Clinical Studies on Lactate and Pyruvate as Indicators of the Severity of Acute Circulatory Failure (Shock)," *Circulation* **41**(6), 989–1001 (1970).
15. M. R. Liebowitz, A. J. Fyer, J. M. Gorman, D. Dillon, I. L. Appleby, G. Levy, S. Anderson, M. Levitt, M. Palij, S. O. Davies, *et al.*, "Lactate provocation of panic attacks. I. Clinical and behavioral findings," *Arch. Gen. Psychiatry* **41**(8), 764–770 (1984).
16. L. B. Gladden, "Lactate metabolism: a new paradigm for the third millennium," *J. Physiol.* **558**(1), 5–30 (2004).
17. B. Kubera, C. Hubold, S. Otte, A. S. Lindenberg, I. Zeiss, R. Krause, M. Steinkamp, J. Klement, S. Entringer, L. Pellerin, and A. Peters, "Rise in Plasma Lactate Concentrations with Psychosocial Stress: A Possible Sign of Cerebral Energy Demand," *Obesity Facts* **5**(3), 384–392 (2012).
18. R. Garjonyte, Y. Yigzaw, R. Meskys, A. Malinauskas, and L. Gorton, "Prussian Blue- and lactate oxidase-based amperometric biosensor for lactic acid," *Sens. Actuators B Chem.* **79**(1), 33–38 (2001).
19. C. Boozer, J. Ladd, S. Chen, Q. Yu, J. Homola, and S. Jiang, "DNA Directed Protein Immobilization on Mixed ssDNA/Oligo(ethylene glycol) Self-Assembled Monolayers for Sensitive Biosensors," *Anal. Chem.* **76**(23), 6967–6972 (2004).
20. G. Suárez, R. J. Jackson, J. A. Spoors, and C. J. McNeil, "Chemical Introduction of Disulfide Groups on Glycoproteins: A Direct Protein Anchoring Scenario," *Anal. Chem.* **79**(5), 1961–1969 (2007).
21. H. Vaisocherová, W. Yang, Z. Zhang, Z. Cao, G. Cheng, M. Piliarik, J. Homola, and S. Jiang, "Ultralow Fouling and Functionalizable Surface Chemistry Based on a Zwitterionic Polymer Enabling Sensitive and Specific Protein Detection in Undiluted Blood Plasma," *Anal. Chem.* **80**(20), 7894–7901 (2008).
22. J. R. Henderson, H. Swalwell, S. Boulton, P. Manning, C. J. McNeil, and M. A. Birch-Machin, "Direct, real-time monitoring of superoxide generation in isolated mitochondria," *Free Radic. Res.* **43**(9), 796–802 (2009).
23. J. R. Henderson, D. A. Fulton, C. J. McNeil, and P. Manning, "The development and in vitro characterisation of an intracellular nanosensor responsive to reactive oxygen species," *Biosens. Bioelectron.* **24**(12), 3608–3614 (2009).
24. G. Suárez, N. Keegan, J. A. Spoors, P. Ortiz, R. J. Jackson, J. Hedley, X. Borrisé, and C. J. McNeil, "Biomolecule Patterning on Analytical Devices: A Microfabrication-Compatible Approach," *Langmuir* **26**(8), 6071–6077 (2010).
25. C. Boero, S. Carrara, G. Del Vecchio, L. Calza, and G. De Micheli, "Highly Sensitive Carbon Nanotube-Based Sensing for Lactate and Glucose Monitoring in Cell Culture," *IEEE Trans. NanoBioscience*, **10**, 59–67 (2011).
26. T. Sikora, G. Istamboulie, E. Jubete, E. Ochoteco, J.-L. Marty, and T. Noguier, "Highly Sensitive Detection of Organophosphate Insecticides Using Biosensors Based on Genetically Engineered Acetylcholinesterase and Poly(3,4-Ethylenedioxythiophene)," *J. Sens.* **2011**, 1–7 (2011).
27. S. Govindarajan, C. J. McNeil, J. P. Lowry, C. P. McMahon, and R. D. O'Neill, "Highly selective and stable microdisc biosensors for l-glutamate monitoring," *Sens. Actuators B Chem.* **178**, 606–614 (2013).
28. G. Kenausis, Q. Chen, and A. Heller, "Electrochemical Glucose and Lactate Sensors Based on "Wired" Thermostable Soybean Peroxidase Operating Continuously and Stably at 37 °C," *Anal. Chem.* **69**(6), 1054–1060 (1997).
29. K. Sirkar, A. Revzin, and M. V. Pishko, "Glucose and Lactate Biosensors Based on Redox Polymer/Oxidoreductase Nanocomposite Thin Films," *Anal. Chem.* **72**(13), 2930–2936 (2000).
30. W. Jia, A. J. Bandodkar, G. Valdés-Ramírez, J. R. Windmiller, Z. Yang, J. Ramírez, G. Chan, and J. Wang, "Electrochemical Tattoo Biosensors for Real-Time Noninvasive Lactate Monitoring in Human Perspiration," *Anal. Chem.* **85**(14), 6553–6560 (2013).
31. W. Putzbach and N. J. Ronkainen, "Immobilization Techniques in the Fabrication of Nanomaterial-Based Electrochemical Biosensors: A Review," *Sensors (Basel)* **13**(4), 4811–4840 (2013).

32. Y.-S. Li, X. Ju, X.-F. Gao, and W. Yang, "A Novel Immobilization Enzyme Lactate Fluorescence Capillary Biosensor," *Chin. J. Anal. Chem.* **37**(5), 637–642 (2009).
33. H. Chen, R. Li, L. Lin, G. Guo, and J.-M. Lin, "Determination of L-ascorbic acid in human serum by chemiluminescence based on hydrogen peroxide-sodium hydrogen carbonate-CdSe/CdS quantum dots system," *Talanta* **81**(4-5), 1688–1696 (2010).
34. W. Chen, L. Hong, A.-L. Liu, J.-Q. Liu, X.-H. Lin, and X.-H. Xia, "Enhanced chemiluminescence of the luminol-hydrogen peroxide system by colloidal cupric oxide nanoparticles as peroxidase mimic," *Talanta* **99**, 643–648 (2012).
35. D. C. Klonoff, "Overview of Fluorescence Glucose Sensing: A Technology with a Bright Future," *J. Diabetes Sci. Tech.* **6**(6), 1242–1250 (2012).
36. U. Resch-Genger, M. Grabolle, S. Cavaliere-Jaricot, R. Nitschke, and T. Nann, "Quantum dots versus organic dyes as fluorescent labels," *Nat. Methods* **5**(9), 763–775 (2008).
37. B. Kalyanaraman, V. Darley-Usmar, K. J. A. Davies, P. A. Dennery, H. J. Forman, M. B. Grisham, G. E. Mann, K. Moore, L. J. Roberts 2nd, and H. Ischiropoulos, "Measuring reactive oxygen and nitrogen species with fluorescent probes: challenges and limitations," *Free Radic. Biol. Med.* **52**(1), 1–6 (2012).
38. G. Suárez, C. Santschi, V. I. Slaveykova, and O. J. F. Martin, "Sensing the dynamics of oxidative stress using enhanced absorption in protein-loaded random media," *Sci. Rep.* **3**, 3447 (2013).
39. V. B. Koman, C. Santschi, and O. J. F. Martin, "Multiscattering-Enhanced Absorption Spectroscopy," *Anal. Chem.* **87**(3), 1536–1543 (2015).
40. G. Suárez, C. Santschi, G. Plateel, O. J. F. Martin, and M. Riediker, "Absorbance enhancement in microplate wells for improved-sensitivity biosensors," *Biosens. Bioelectron.* **56**, 198–203 (2014).
41. V. Koman, G. Suárez, C. Santschi, V. J. Cadarso, J. Brugger, N. von Moos, V. I. Slaveykova, and O. J. F. Martin, "A portable microfluidic-based biophotonic sensor for extracellular H₂O₂ measurements," *Proc. SPIE* **8572**, 857218 (2013).
42. V. B. Koman, C. Santschi, N. R. von Moos, V. I. Slaveykova, and O. J. F. Martin, "Portable oxidative stress sensor: dynamic and non-invasive measurements of extracellular H₂O₂ released by algae," *Biosens. Bioelectron.* **68**, 245–252 (2015).
43. F. S. Ligler and C. A. R. Taitt, *Optical biosensors: present and future* (Gulf Professional Publishing, 2002).
44. E. A. Drew, "Uptake and metabolism of exogenously supplied sugars by brown algae," *New Phytol.* **68**(1), 35–43 (1969).
45. A. Grossman, "In the Grip of Algal Genomics," in *Transgenic Microalgae as Green Cell Factories*, R. León, A. Galván, and E. Fernández, eds. (Springer New York, 2007), pp. 54–76.
46. R. A. Pelroy, R. Rippka, and R. Y. Stanier, "Metabolism of glucose by unicellular blue-green algae," *Arch. Mikrobiol.* **87**(4), 303–322 (1972).
47. P. Xie, I. Fujii, J. Zhao, M. Shinohara, and M. Matsukura, "A Novel Polysaccharide Compound Derived from Algae Extracts Protects Retinal Pigment Epithelial Cells from High Glucose-Induced Oxidative Damage in Vitro," *Biol. Pharm. Bull.* **35**(9), 1447–1453 (2012).
48. W. Dröge, "Free Radicals in the Physiological Control of Cell Function," *Physiol. Rev.* **82**(1), 47–95 (2002).
49. G. Suarez, C. Santschi, S. Dutta-Gupta, L. Juillerat-Jeanneret, and O. J. F. Martin, "Biophotonic tool for sensing the dynamics of H₂O₂ extracellular release in stressed cells," *Proc. SPIE* **8229**, 822908 (2012).
50. W. D. Butt and D. Keilin, "Absorption spectra and some other properties of cytochrome c and of its compounds with ligands," *Proc. R. Soc. Lond. B Biol. Sci.* **156**(965), 429–458 (1962).
51. L. Huang, S. J. Maerkl, and O. J. Martin, "Integration of plasmonic trapping in a microfluidic environment," *Opt. Express* **17**(8), 6018–6024 (2009).
52. S. A. Gerber, C. R. Scott, F. Turecek, and M. H. Gelb, "Analysis of Rates of Multiple Enzymes in Cell Lysates by Electrospray Ionization Mass Spectrometry," *J. Am. Chem. Soc.* **121**(5), 1102–1103 (1999).
53. C. A. Rowe, S. B. Scruggs, M. J. Feldstein, J. P. Golden, and F. S. Ligler, "An array immunosensor for simultaneous detection of clinical analytes," *Anal. Chem.* **71**(2), 433–439 (1999).
54. J. Homola, H. B. Lu, G. G. Nenninger, J. Dostálek, and S. S. Yee, "A novel multichannel surface plasmon resonance biosensor," *Sens. Actuators B Chem.* **76**(1-3), 403–410 (2001).
55. A. Liesener and U. Karst, "Monitoring enzymatic conversions by mass spectrometry: a critical review," *Anal. Bioanal. Chem.* **382**(7), 1451–1464 (2005).
56. C. G. Pheaney, A. R. Arnold, M. A. Grodick, and J. K. Barton, "Multiplexed electrochemistry of DNA-bound metalloproteins," *J. Am. Chem. Soc.* **135**(32), 11869–11878 (2013).
57. M.-C. Shin, H. C. Yoon, and H.-S. Kim, "In situ biochemical reduction of interference in an amperometric biosensor with a novel heterobilayer configuration of polypyrrole/glucose oxidase/horseradish peroxidase," *Anal. Chim. Acta* **329**(3), 223–230 (1996).
58. L. Michaelis, M. L. Menten, K. A. Johnson, and R. S. Goody, "The original Michaelis Constant: Translation of the 1913 Michaelis-Menten Paper," *Biochemistry* **50**(39), 8264–8269 (2011).

1. Introduction

Real-time information on metabolic processes in cell cultures provides important insights into cell state and cellular mechanisms [1, 2]. Furthermore, metabolome data can be used for medical diagnostics and health monitoring [3, 4]. Many researchers focus their attention on

the detection of specific metabolites such as cholesterol, glutamate, glucose and lactate [5, 6]. In particular, the detection of glucose is interesting in the context of the biochemical cycle of energy harvesting, diabetes pathology, as well as fermentation control in food industry [7–11]. Lactate, in addition, acts as a cerebral energy substrate and as a product in anaerobic metabolism during muscle contraction, malnutrition and hypoxia [12–17]. Thus, a sensitive method for the continuous and simultaneous detection of several such metabolites will broaden our understanding of cell biochemistry and have a significant impact on medical diagnostics.

Currently, mainly electrochemical biosensors are used for the extracellular detection of both glucose and lactate. Large efforts have been put into the design of those sensors, especially structuring the electrodes with mediators, gels, polymeric matrices and various nanomaterials [18–27]. Most reported methods are based on sample collection prior to laboratory analysis and are, therefore, end-point assays [28, 29]. As an exception, Jia *et al.* have recently presented a real-time lactate biosensor with millimolar limit of detection (LOD) [30]. Yet, electrochemical sensors suffer from electrode fouling and lack of long-term stability [31]. Chemiluminescent and fluorescent biosensors represent another very sensitive way of sensing glucose and lactate [32–35]; although their use for continuous measurements remains problematic because of their limited stability and deactivation through photobleaching [36]. Additionally, often invasive, these sensors can interfere with the redox cycles of cells [36, 37].

Here, we introduce a non-invasive, multiscattering-enhanced and real-time biosensor with sub-micromolar LODs for H₂O₂, lactate and glucose measurements that relies on a porous membrane. The refractive index of porous membranes exhibits spatial variations leading to multiple scattering of light and consequently to enhanced optical path lengths [38–40]. Such membranes can, therefore, be used to enhance the response of an optical reporter to exposure to specific analytes. In this work, we use cyt *c* as reporter: its absorption spectrum reflects the average oxidation of its heme group and provides a sensing element for the detection of hydrogen peroxide (H₂O₂) in the surrounding medium down to nanomolar concentrations [38, 41, 42]. We will show that this concept enables the detection of many other analytes (especially here glucose and lactate) that undergo enzymatic reactions with H₂O₂ as reaction product. Furthermore, this optical detection approach enables continuous and multiplexed measurements for several analytes, while the integration of our optical probes into a microfluidic chip suppresses chemical interferences between probes and enables automatic and differential measurement procedures [43].

As an example to demonstrate the performance of the biosensor, we measure the effects of exogenously supplied glucose on the algae *Chlamydomonas reinhardtii* using the developed biosensor. *C. reinhardtii* is a widespread microorganism that generates glucose as one of the final products of photosynthesis [44, 45]. The study of glucose uptake by algae opens new perspectives for gaining insights into several biochemical processes: (1) the algae ability to accumulate glucose, (2) whether glucose feeding can substitute light harvesting and (3) the glucose metabolic pathways [44, 46]. It is known that large doses of glucose may misbalance the cells homeostasis and harm them [47]. To assess the physiological state of algae, we also detect extracellular H₂O₂ using the multiplexing feature of our biosensor platform [38]. H₂O₂ is one of the most stable reactive oxygen species, which are overproduced by cells during oxidative stress events [48], and its detection provides information on cell homeostasis.

2. Experimental section

2.1. Preparation of sensing spots

Aqueous droplets containing cyt *c* (4 mM) were picked up with a microarray robot (QArray2, Genetix) from a 384-well plate with a 5 nl delivery-volume spotting pin (946MP8XB, Arrayit) and subsequently deposited onto the membranes (GSWP 220 nm, Millipore), which

were placed on a glass substrate (Fig. 1(a)). Immediately after deposition, the cyt *c* spots were exposed to vaporous glutaraldehyde for 1 h. The resulting crosslinked spots were immersed into water and stored at 4 °C prior use (experiments have shown that the spots could be stored in those conditions for at least 7 days). During the crosslinking process the spots were kept under 100% relative humidity in order to avoid drying, which would denature the heme protein. For the detection of lactate, respectively glucose, hybrid spot mixtures of cyt *c* with different amounts of the corresponding enzymes (lactate oxidase, respectively glucose oxidase) were deposited following the same procedure. All chemicals were purchased from Sigma Aldrich and the solutions were prepared with deionized water.

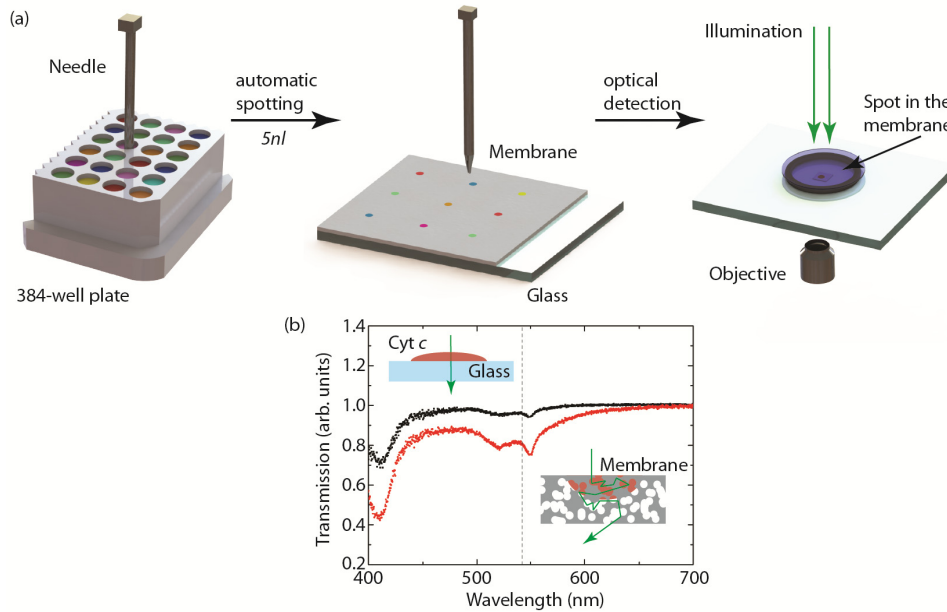


Fig. 1. (a) Solutions containing cyt *c* + enzyme mixtures in microliter well-plates are automatically spotted onto a porous membrane using a microarray robot. The resulting crosslinked spots have a diameter of approx. 600 μm and are spectrally analyzed in transmission. (b) Optical transmission of 20 pmol cyt *c* spots printed on glass (black) or on a porous membrane (red). The insets show schematic of light propagation (green arrow) through samples. The dashed line corresponds to the wavelength $\lambda = 542 \text{ nm}$.

2.2. Optical measurements and oxidative state analysis

For carrying out the sensing experiments, sensing spots and solution of interest were introduced into the measurement chamber (60 μl , O-ring delimited, unless stated otherwise) and placed on an inverted microscope (Olympus IX 71). Subsequently, the absorption spectra were recorded in transmission mode under white-light illumination using an objective (UPlanFL 20x, Olympus, NA = 0.41) and a grating spectrometer (Triax 550, Horiba Scientific) equipped with a liquid nitrogen cooled CCD camera (Symphony, Horiba Scientific). The power of the light at the sample was 10 $\mu\text{W}/\text{cm}^2$ at a wavelength $\lambda = 550 \text{ nm}$.

The change in the oxidation state of cyt *c* was determined from its optical spectrum [41, 49]. The absorption peak at $\lambda = 550 \text{ nm}$ is particularly sensitive to a change in the oxidation state, whereas at $\lambda = 542 \text{ nm}$ and $\lambda = 556 \text{ nm}$ the absorption spectrum remains unchanged. Therefore, the absorbance A at those wavelengths can be used as reference for spectrum analysis. To quantify the oxidation state, an oxidation state coefficient ϕ calculated from the measured optical spectrum is introduced [42]:

$$\varphi = \frac{A_{550} / A_{542} - A_{550}^{ox} / A_{542}^*}{A_{550}^{red} / A_{542}^* - A_{550}^{ox} / A_{542}^*}, \quad (1)$$

where A_{550} and A_{542} are the measured cyt *c* absorbance at $\lambda = 550$ and $\lambda = 542$ nm, respectively. The coefficients A_{550}^{ox} , A_{550}^{red} and A_{542}^* are values taken from the literature, representing the absorbance for the oxidized and reduced state at $\lambda = 550$ nm, and the absorbance at $\lambda = 542$ nm, respectively [50]. The values of A_{550} and A_{542} are deduced from the light intensity measured at the corresponding wavelength using Beer-Lambert's law: $A = -\log(I / I_0)$ where I , respectively I_0 , refers to the light intensity measured after the light has passed through the membrane in the presence, respectively in the absence, of cyt *c*.

The cyt *c* located in the membrane absorbs light more efficiently than the same amount of cyt *c* deposited on a flat glass substrate (Fig. 1(b)). As the absorption A of cyt *c* does not depend on its oxidative state at $\lambda = 542$ nm, the enhancement factor f is defined as the ratio between A_{542} for a spot in the membrane and A_{542} for a spot situated on the glass. For the 20 pmol cyt *c* spots used in our experiments f is 4.5 ± 1.2 . This amplifying effect is caused by two factors: (1) diffidence of the drops on the glass surface forming a thin layer ($<10 \mu\text{m}$), which results in a small optical thickness in that case; (2) light scattering taking place in the pores of the membrane, which enhances the optical path length. Similar values of f are observed for mixtures containing 20 pmol cyt *c* and different enzymes where the enhancement is not affected by the enzyme concentration (data not shown).

2.3. Microfluidic chip

The 2-layered microfluidic chip was fabricated in PDMS using molds that were made with a standard photolithography technique [51]. Briefly, the bottom PDMS layer (100 μm thickness) was deposited by spin-coating PDMS at 500 rpm for 40 s, followed by manual hole cutting to accommodate the sensing spots. This layer serves as planarization layer. The top layer (5 mm thickness) contained the microfluidic channels (0.3 mm \times 0.6 mm cross section) and a 3 mm wide chamber for experiments with cells. It was prepared by pouring the appropriate amount of PDMS onto the mold. Sensing spots were inserted into the bottom layer and aligned with microfluidic channels as will be explained later in the text. The whole system was clamped in a metallic holder with the possibility of being disassembled to exchange the substrate with the sensing spots. Injecting and rinsing of analytes was performed by applying a constant flow of 0.2 mm/sec using a liquid pump (Xcalibur, Tecan).

2.4. Algae culture

The green alga *C. reinhardtii* strain (CPCC 11) was provided by the Canadian Phycological Culture Center. Axenic cultures were grown in diluted Tris-Acetate-Phosphate (TAP) liquid growth medium and maintained in an incubator (Infors, Bottmingen, Switzerland) at 20 °C with a 24 h illumination regime (114.2 $\mu\text{mol}\cdot\text{phot}/(\text{m}^2\cdot\text{s})$) and constant rotary shaking (120 rpm). The algal culture was grown to a density of ca. 2×10^6 cells/ml. Prior to each experiment, algae were harvested by centrifugation (3000 rpm, 5 min), rinsed with and subsequently transferred to deionized water.

3. Results and discussion

3.1. Glucose and lactate detection

Control experiments with glucose and lactate revealed no interaction with cyt *c*. The oxidation state coefficient φ remains constant when a cyt *c* sensing spot (20 pmol) is placed into the chamber containing 440 μM of glucose (Fig. 2(a)). After addition of glucose oxidase (GOx, 500 U/ml), the glucose is catalytically converted into gluconolactone and H_2O_2 . The latter gradually oxidizes cyt *c*, decreasing the oxidation state coefficient φ . Further control

experiments confirmed that GOx does not react with cyt *c*. Similarly to glucose, the presence of 24 μM of lactate does not induce any changes in the oxidation state of cyt *c* (Fig. 2(b)). However, the subsequent addition of 2.5 U/ml lactate oxidase (LOx) results in an oxidation of the cyt *c* in the spot. In contrast to GOx, LOx alone slightly oxidizes cyt *c*, changing ϕ from 0.25 to 0.16 within 30 min. (see the green curve in Fig. 2(b)).

Since the presence of enzymes in the solution can interfere with cyt *c*, we prepared hybrid spots containing cyt *c* and the corresponding enzyme inside the spot. In such a configuration the H_2O_2 conversion and detection occur locally, which significantly reduces the amount of enzyme required. Additionally, since both cyt *c* and the corresponding enzyme are immobilized during crosslinking, such a configuration also eliminates the dynamic direct interaction between the two. In that case, 0.01 U of GOx, respectively 1.25×10^{-4} U of LOx, in the 5 nl printed sensing spot are sufficient to sensitively detect glucose, respectively lactate (Fig. 2(c) and 2(d)). The calibration curves for these hybrid spots, which show the difference between the initial and the final oxidation state coefficients $\Delta\phi = \phi_{\text{initial}} - \phi_{\text{final}}$ after 30 min, are shown in Fig. 2(e) and 2(f). Even though the detection interval can be chosen arbitrarily, here we choose 30 min, which represents the average waiting time for many optical bioassays [43]. From these data we deduce a LOD of 9.6 μM for lactate and 1.1 μM for glucose for the above mentioned enzyme concentrations. The LOD decreases when one increases the amount of enzyme: the LOD for lactate is as small as 0.24 μM with 2.5×10^{-3} U of LOx, Fig. 2(f); while the LOD for glucose is 0.11 μM with 0.1 U of GOx, Fig. 2(e). To the best of our knowledge, these values are at least one order of magnitude lower than those reported in the recent literature [25].

3.2. Multiplexing measurements

The possibility of multiplexed analysis allows for the simultaneous detection of several analytes and can also be used to reduce background contributions and obtain a more reliable statistics [52–56]. A multiplexed experiment is shown in the right top of Fig. 3, where two sensing spots spaced 1 mm apart are visible in the measurement chamber; the spots can include only cyt *c* or a mixture of cyt *c* and enzyme. In order to perform multiplexed measurements, absorption spectra from different sensing spots must be recorded simultaneously, which requires a precise alignment in the microscope, while additional markings on the membrane are used to identify the sensing spots (photo in Fig. 3).

Enzymatic reactions result in the production of H_2O_2 in the vicinity of the sensing spot and – by diffusion – in an increased concentration in the solution as well, which can interfere with neighboring sensing spots. To investigate such interferences, we loaded the experimental chamber with different combinations of pairs of sensing spots and exposed them to H_2O_2 , glucose and lactate (Fig. 3(a)-3(c)).

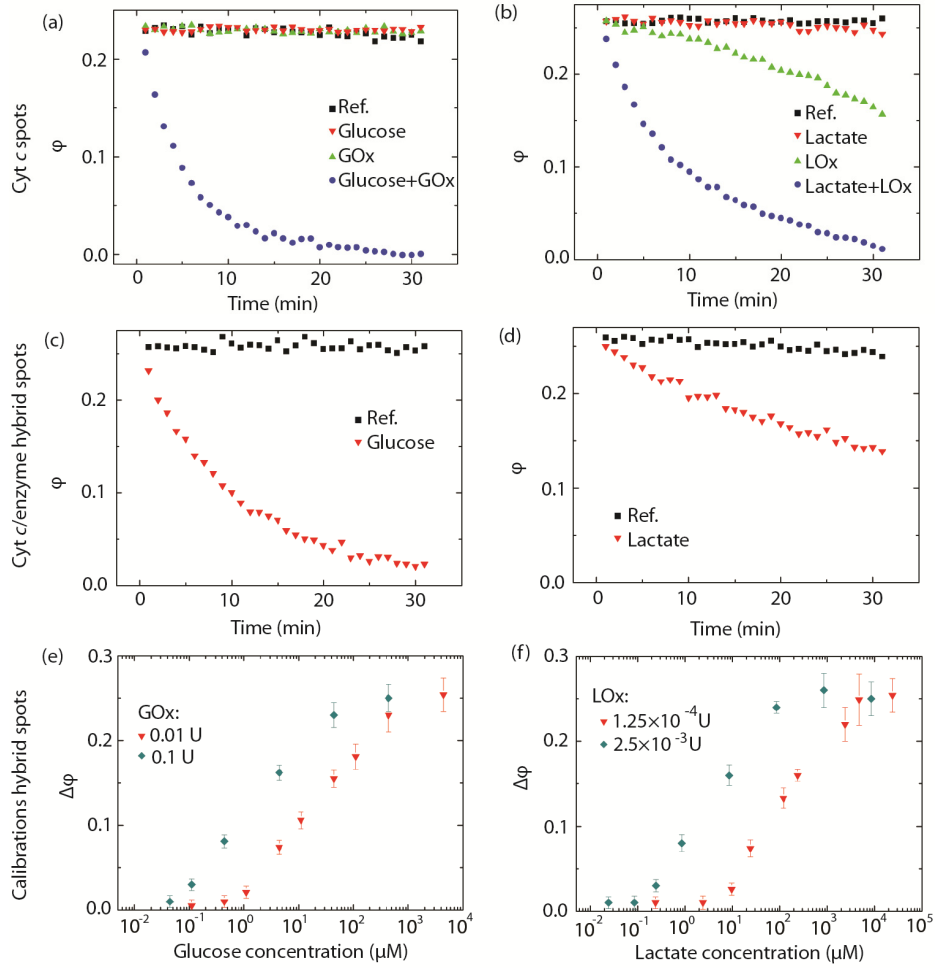


Fig. 2. (a) Time evolution of the oxidation state coefficient $\phi(t)$ for a 20 pmol cyt *c* sensing spot exposed to water (Ref.), to a 440 μM glucose solution in water (Glucose), to a 500 U/ml GOx solution in water (GOx), or to a solution with 440 μM glucose and 500 U/ml GOx in water (Glucose + GOx). (b) Time evolution of the oxidation state coefficient $\phi(t)$ for a 20 pmol cyt *c* sensing spot exposed to water (Ref.), to a 24 μM lactate solution in water (Lactate), to a 2.5 U/ml LOx solution in water (LOx), or to a solution with 440 μM glucose and 2.5 U/ml LOx in water (Lactate + LOx). (c) Time evolution of the oxidation state coefficient $\phi(t)$ for a hybrid sensing spot containing 20 pmol cyt *c* and 0.01 U GOx exposed to water (Ref.) or to a 440 μM glucose solution in water (Glucose). (d) Time evolution of the oxidation state coefficient $\phi(t)$ for a hybrid sensing spot containing 20 pmol cyt *c* and 1.25×10^{-4} U LOx exposed to water (Ref.) or to a 24 μM lactate solution in water (Lactate). (e) Calibration curve: response of the hybrid sensing spot in (c) after 30 min. as a function of the glucose concentration, for two different concentrations of GOx in the sensing spot: 0.1 U and 0.01 U. (f) Calibration curve: response of the hybrid sensing spot in (d) after 30 min. as a function of the lactate concentration, for two different concentrations of LOx in the sensing spot: 1.25×10^{-4} U and 2.5×10^{-3} U. The error bars in (e) and (f) represent the standard deviation over 3 measurements.

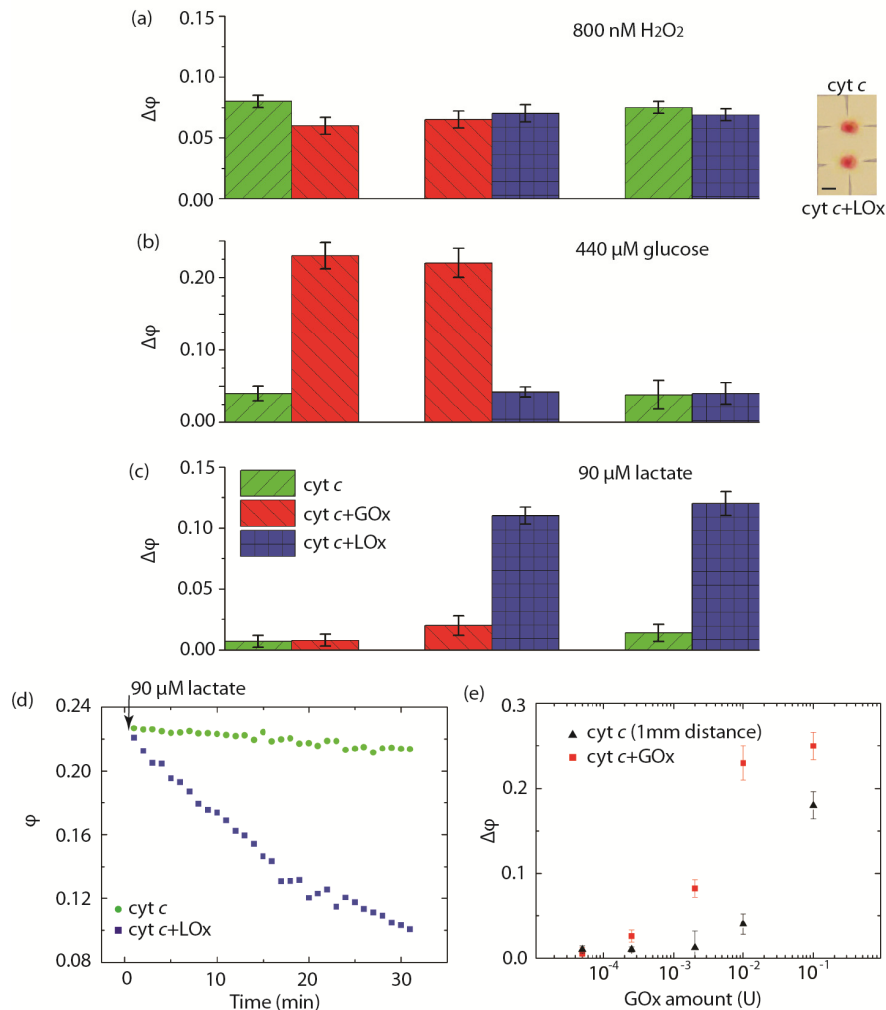


Fig. 3. Multiplexed measurements using different pairs of sensing spots in the O-ring measurement chamber (photo to the right of panel a, the distance between the spots is 1 mm and the scale bar is 0.5 mm): green: spot with 20 pmol cyt *c*; red: 20 pmol cyt *c* + 0.01 U GOx; blue: 20 pmol cyt *c* + 1.25×10^{-4} U LOx. Response after 30 min. of the three different pairs of sensing spots to (a) 800 nM H_2O_2 , (b) 440 μM glucose and (c) 90 μM lactate. (d) Kinetics of the multiplexed oxidation state coefficient ϕ for a pair of spots (green and blue) exposed to 90 μM lactate. (e) Calibration curve: difference of the oxidation state coefficient after 30 min. $\Delta\phi$ for different amounts of GOx in hybrid spots containing 20 pmol cyt *c* + GOx, after exposure to 440 μM of glucose; the response of a spot containing only 20 pmol cyt *c*, 1 mm away from the hybrid spot is also shown (crosstalks). The error bars represent the standard deviation over 3 measurements.

The sensing spots contain either 20 pmol cyt *c* (green in Fig. 3), or 20 pmol cyt *c* and 1.25×10^{-4} U LOx (blue in Fig. 3), or 20 pmol cyt *c* and 0.01 U GOx (red in Fig. 3) and are always exposed in pairs, which provides quantitative measurements for the crosstalks between them. In the first series of experiments, reported in Fig. 3(a), we expose the three different possible combinations of sensing spots to 800 nM H_2O_2 . Hybrid spots containing both cyt *c* and an enzyme exhibit a slightly lower response to H_2O_2 as compared to the spot containing only cyt *c*; probably because the presence of enzyme hinders the access of analytes to the cyt *c*. We then repeat these experiments, exposing the pairs of sensing spots to 440 μM glucose (Fig.

3(b)), or 90 μM lactate (Fig. 3(c)). As anticipated, when glucose reacts with the *cyt c* + GOx hybrid sensing spot, the enzymatically produced H_2O_2 also oxidizes the neighboring *cyt c* sensing spot, which $\Delta\phi$ increases from 0.038 to 0.042, Fig. 3(b). This crosstalk is more pronounced when lactate reacts with the *cyt c* + LOx hybrid sensing spot; in that case, the $\Delta\phi$ of the neighboring *cyt c* sensing spot increases to 0.014, as compared to 0.007 when no reaction happens in the hybrid spot, Fig. 3(c) and 3(d).

The sensitivity of such a hybrid spot depends on the conversion rate to H_2O_2 , which in turn depends on the amount of enzyme. To investigate this, we have exposed hybrid sensing spots containing different amounts of GOx to a constant glucose concentration of 440 μM . Figure 3(e) indicates that the difference $\Delta\phi$ of oxidation state coefficient after 30 min. increases with the GOx amount. Thus, adjusting the amount of GOx controls the sensitivity and dynamic range of the sensor. Unfortunately, increasing the amount of enzymes also increases the enzymatically produced H_2O_2 , which augments the crosstalks between neighboring sensing spots. A simple way to reduce crosstalks would be to increase the distance between neighboring spots [56], or to use a hetero bilayer configuration [57].

3.3. Microfluidic chip

A more drastic way to suppress interference effects is to integrate the sensing spots in a 2-layer microfluidic chip as described in the methods section (Fig. 4(a)). The sensing spots are introduced into the bottom layer and aligned with respect to the microfluidic channels in the top layer, one sensing spot per channel, so that enzymatically produced H_2O_2 remains within the channel and does not interfere with another sensing spot.

As shown in Fig. 3, multiplexed experiments performed in the O-ring measurement chamber interfere; in contrast, this is not at all the case in the microfluidic chip. This is visible in Fig. 4(b), where we compare measurements performed in the microfluidic chip with a 0.2 mm/sec flow (noted with asterisks) with measurements in the chamber delimited by an O-ring. Even for the very high lactate concentration used here (almost 10x higher than the concentration used in Fig. 3(d)), the response of the pure *cyt c* sensing spot remains almost constant (blue inverted triangles in Fig. 4(b)), while lactate is well measured by the hybrid spot (green triangles in Fig. 4(b)). Such a microfluidics approach could be used to detect a larger number of analytes, by merely increasing the number of channels and sensing spots in the chip, Fig. 4(c).

In the following, we will perform continuous measurements of the algae response to a specific analyte. To trace the reaction dynamics, these experiments have to be performed in the static regime. Additionally, microfluidic channels must be used to suppress crosstalks. To account for these two points, we developed the following procedure: the algae are mixed with the analyte, then the mixture is injected into the microfluidic chip and, finally, the flow is stopped when the mixture reaches the sensing spots. Since the microfluidic channel has a very small volume (approx. 0.15 μl), the reaction of the analyte with the sensing spot can deplete the concentration of the former. To avoid such an interference, we included a 10 μl cell chamber in the microfluidic chip, which acts as a buffer volume [42]. The cell chamber significantly increases the total volume of the system and the diffusion effectively repletes the sensing channels with H_2O_2 . Similarly to the experiments in the flow regime, sensing spots in separate channels do not experience any crosstalk even in the static regime (data not shown). Overall, both the cell chamber and the separated microfluidic channels are crucial design elements in these experiments.

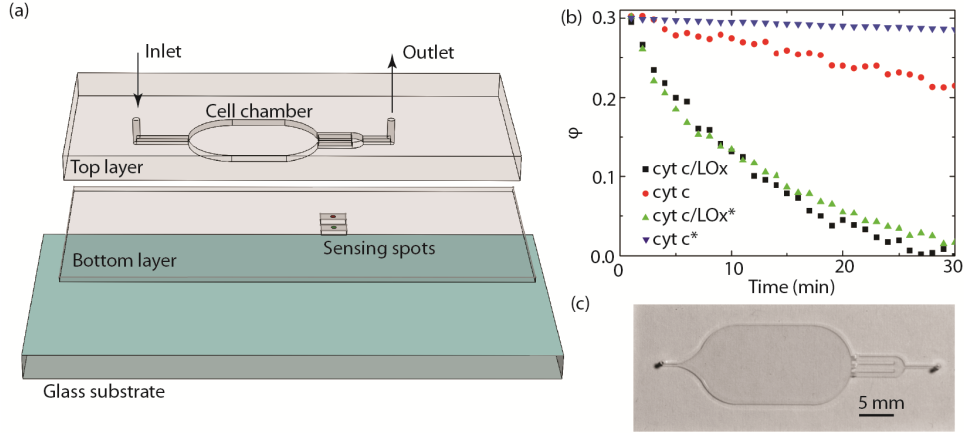


Fig. 4. (a) Schematic of the microfluidic chip consisting of a glass substrate, a bottom PDMS layer containing the sensing spots and a top PDMS layer with channels and cell chamber. (b) Comparison of crosstalks between two sensing spots, one with 20 pmol cyt *c* and another one with 20 pmol cyt *c* + 2.5×10^{-3} U LOx exposed to 850 μM lactate. The asterisks denote the experiment performed in the microfluidic chip with a 0.2 mm/sec flow; the other experiment is performed in the O-ring chamber. (c) Picture of a top layer with three microfluidic channels coming out of the cell chamber.

3.4. Time-dependent rate determination

Till now, we have detected constant concentrations of analytes. However, in biological processes the release or uptake of biomarkers has a time-dependent rate. In this case, the concentration $C_{H_2O_2}$ of H_2O_2 in the proximity of the sensing spot at a given time t can be determined as follows [42]:

$$C_{H_2O_2} = -\frac{d\varphi/dt}{k\varphi}, \quad (2)$$

where k ($= 0.24 \text{ min}^{-1} \cdot \mu\text{M}^{-1}$) is the interaction constant for the oxidation of cyt *c* by H_2O_2 in water.

To link $C_{H_2O_2}$ with the analyte (glucose or lactate) concentration in the solution $C_a(t)$, let us look into the reaction kinetics. In hybrid spots, the reaction of the analyte with the enzyme follows the Michaelis–Menten kinetics [58]. The resulting enzymatically-produced H_2O_2 partially reacts with cyt *c*, while the rest diffuses throughout the chamber. The consumed analyte creates a concentration gradient at the proximity of the sensing spot, where the analyte concentration can differ from $C_a(t)$. In general, an exact relation between $C_{H_2O_2}$ and $C_a(t)$ in this system can be very complex. However, since the measurements with hybrid spots for a constant analyte concentration (Fig. 2(c) and 2(d)) fit well with a single exponential function ($\varphi = e^{-C_{H_2O_2}kt}$, data not shown), $C_{H_2O_2}$ remains constant in time. This indicates that the system quickly (in less than 1 min) reaches a steady state: enzymatically-produced H_2O_2 balances the diffused one. Therefore, at a given time t , $C_{H_2O_2}$ only depends on C_a , not on the previous state of the system. We can write $C_{H_2O_2} = f(C_a)$ and, comparing the calibration curves $\Delta\varphi(C_a)$ of the hybrid spots with that of H_2O_2 taken from [42], we have found that a second order polynomial expansion expresses the correlation $C_a = f^{-1}(C_{H_2O_2})$ very well:

$$C_a = f^{-1}(C_{H_2O_2}) = aC_{H_2O_2}^2 + bC_{H_2O_2} + d. \quad (3)$$

The resulting coefficients obtained from fitting the experimental data are summarized in Table 1, where both $C_{H_2O_2}$ and C_a are expressed in micromolars. Higher order expansion terms are insignificant. Since Eqs. (2) and (3) establish a link between $\varphi(t)$ and $C_a(t)$, we can now obtain quantitative data for the analyte (lactose or glucose) concentration.

Let us emphasize that experiments performed with living organisms are often accompanied by an oxidative stress, leading to the production of H_2O_2 by the organisms under study. The multiplexed technique presented here becomes extremely handy in that case, as it makes possible isolating the oxidative stress-produced H_2O_2 from that produced enzymatically. Using a pair of sensing spots that measure: analyte + H_2O_2 (spot 1) or H_2O_2 (spot 2), we first use Eq. (2) to extract $C_{H_2O_2}$ for both spots. Next, we subtract $C_{H_2O_2}(2)$ of the second spot from that of the first spot $C_{H_2O_2}(1)$. Finally, C_a can be calculated from Eq. (3) using the obtained difference $C_{H_2O_2}(1-2)$. This will be utilized in the next section to determine glucose uptake in aquatic microorganisms.

Table 1. Fitting coefficients for Eq. (3) of hybrid spots (only valid in the 0.1–1000 μ M analyte range).

	0.1 U GOx	0.01 U GOx	2.5×10^{-3} U LOx	1.25×10^{-4} U LOx
<i>a</i>	-0.16	-1.13	-0.63	-1.66
<i>b</i>	2.24	2.55	2.43	2.51
<i>d</i>	-0.31	0.83	0.03	1.62

3.5. Uptake of exogenously supplied glucose

To study the uptake of glucose on the green alga *C. reinhardtii*, we inject a mixture of glucose and algae into the microfluidic chip. Once this mixture reaches the cell chamber, the flow is stopped for the time of the experiment. The multiplexed measurements are performed with two spots: a cyt *c* spot to detect the stress-related H_2O_2 (Fig. 5(a)) and a hybrid spot (cyt *c* + GOx), which is sensitive to both glucose and H_2O_2 (Fig. 5(b)). During our experiments, no H_2O_2 was detected (Fig. 5(c)), suggesting that the algae are not stressed by the presence of glucose and, therefore, only glucose oxidizes the hybrid spot. Using the approach developed in the previous section and the data in Table 1, we can obtain the concentrations C_a in the solution for glucose (Fig. 5(d)). Due to the uptake by algae, the glucose concentration drops from the initial concentration of 8 μ M to 5 μ M within 1 h (red data in Fig. 5(d)). Control experiments without algae revealed a stable glucose concentration in the cell chamber (green data in Fig. 5(d)). Comparing the external volume of the chamber (10 μ l) with the internal volume of all algae in the experiment (approx. 0.033 μ l), we obtain a 300:1 volume ratio. Therefore, *C. reinhardtii* internalize the equivalent of 900 μ M (1.5 fmole/cell) of glucose within 1 h. This glucose uptake is similar to blue algae *Aphanocapsa 6714* that can uptake as much as 500 μ M (0.8 fmole/cell) of glucose within one hour by converting it into CO_2 [46]. Overall, our experiments demonstrate the possibility of sensitive, multiplexed and continuous measurements, which can be further applied to more sophisticated mechanistic studies of cellular processes.

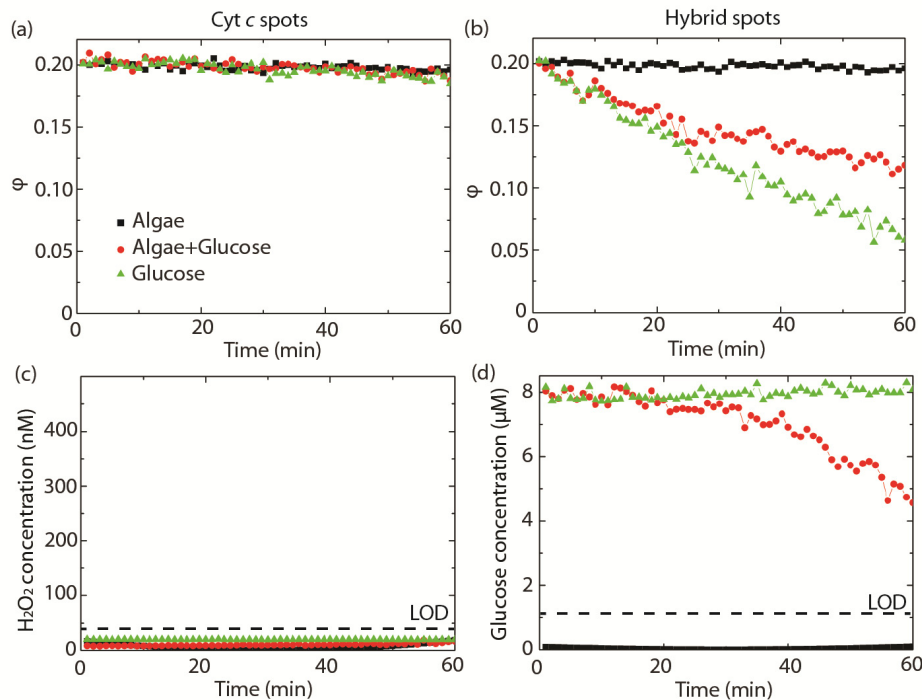


Fig. 5. Glucose uptake ($8 \mu\text{M}$) and H_2O_2 release by *C. reinhardtii* (2×10^6 cells/ml). Multiplexed measurements in microfluidics using (a) a spot with 20 pmol cyt *c* and (b) a hybrid spot with 20 pmol cyt *c* + 0.01 U GOx. Calculated concentrations of (c) H_2O_2 and (d) glucose using Eqs. (2) and (3). The same symbols are used for all panels. Limit of detection (LOD) is 40 nM for cyt *c* spots (taken from [42]) and 1.1 μM for hybrid spots.

4. Summary

We have presented a new sensitive approach for the detection and the continuous monitoring of glucose and lactate. These two analytes are enzymatically converted to H_2O_2 , which is, in turn, detected via the oxidation of cyt *c*. Such conversions take place locally thanks to the corresponding enzymes, which are incorporated in the sensing spot and fabricated by contact spotting technique in a very reliable and reproducible fashion. Extremely low LODs of 240 and 110 nM have been achieved for glucose and lactate, respectively. By integrating such sensing elements into a microfluidic chip, we were able to efficiently suppress crosstalk between different sensing spots and to monitor in real-time the metabolism of *C. reinhardtii*. As demonstrated by the study of glucose uptake in such algae, the proposed method provides a non-invasive, label-free way to measure simultaneously in real-time the by-products of several cellular processes. Furthermore, such a biosensor is fast, cheap and easy to fabricate and has the potential to become a promising candidate for medical diagnostics and healthcare monitoring.

Acknowledgments

This work is supported by the Swiss National Science Foundation in the framework of the Swiss National Research Program NRP 64 project no. 406440-131280/1. We are indebted to Prof. Vera I. Slaveykova and Nadia R. von Moos for providing the algae used in the experiments and training us on how to cultivate them. We are very grateful to Prof. Sebastian Maerkl for the utilization of the microarray robot and to Prof. Christof Holliger for access to the algae incubator. It is a pleasure to acknowledge stimulating discussions with Dr. S. Dutta-Gupta.